Growth of large-area atomically thin MoS_2 film via ambient pressure chemical vapor deposition

Caiyun Chen,[1] Hong Qiao,[1] Yunzhou Xue,[1] Wenzhi Yu,[1] Jingchao Song,[2] Yao Lu,[1] Shaojuan Li,[1] and Qiaoliang Bao[1,2,*]

[1]*Institute of Functional Nano and Soft Materials (FUNSOM), Jiangsu Key Laboratory for Carbon-Based Functional Materials and Devices, and Collaborative Innovation Center of Suzhou Nano Science and Technology, Soochow University, Suzhou 215123, China*
[2]*Department of Materials Engineering, Monash University, Clayton, Victoria 3800, Australia*
**Corresponding author: qlbao@suda.edu.cn*

Received January 12, 2015; revised March 7, 2015; accepted March 8, 2015;
posted March 11, 2015 (Doc. ID 232329); published May 7, 2015

Atomically thin MoS_2 films have attracted significant attention due to excellent electrical and optical properties. The development of device applications demands the production of large-area thin film which is still an obstacle. In this work we developed a facile method to directly grow large-area MoS_2 thin film on SiO_2 substrate via ambient pressure chemical vapor deposition method. The characterizations by spectroscopy and electron microscopy reveal that the as-grown MoS_2 film is mainly bilayer and trilayer with high quality. Back-gate field-effect transistor based on such MoS_2 thin film shows carrier mobility up to 3.4 $cm^2\ V^{-1}\ s^{-1}$ and on/off ratio of 10^5. The large-area atomically thin MoS_2 prepared in this work has the potential for wide optoelectronic and photonic device applications.

OCIS codes: (310.3840) Materials and process characterization; (310.6188) Spectral properties; (310.6845) Thin film devices and applications; (310.6870) Thin films, other properties.
http://dx.doi.org/10.1364/PRJ.3.000110

1. INTRODUCTION

Atomic-layered molybdenum disulfide (MoS_2), a new two-dimensional (2D) material, has gained intense attention due to its outstanding electrical and optical properties [1–5]. When bulk MoS_2 is reduced to monolayer sheet, an indirect-to-direct bandgap transition occurs, leading to extremely high quantum efficiency for light emission [6,7]. Compared with graphene, MoS_2 has a visible bandgap to allow the field-effect transistors based on this material to be effectively switching off. Moreover, the carrier mobility is impressively high, up to 400 $cm^2\ V^{-1}\ s^{-1}$ in theory [8] and 45 $cm^2\ V^{-1}\ s^{-1}$ demonstrated in experiments [2] for monolayer MoS_2. In order to fulfill the demands for device applications, substantial efforts have been devoted into synthesize atomically thin MoS_2 film, including micromechanical exfoliation [4,5,9,10], liquid exfoliation [11–13], and physical vapor deposition [14]. However, MoS_2 films are often limited to their micrometer size, which hinders large-scale device applications. Hence, it is critical to develop practical methods to grow large-area MoS_2 thin film aiming for device fabrications.

Similar to the growth of large-area graphene film, chemical vapor deposition (CVD) has been successfully applied to synthesize large-area MoS_2 film. Zhan *et al.* [15] reported the production of large-area few-layer MoS_2 film through sulfiding the Mo/SiO_2 substrate but the thin films possess poor quality. Alternatively, the thermal decomposition of $(NH_4)_2MoS_4$ [16] in the presence of mixed gas could also induce large-area MoS_2 thin film; however, the pre-deposition of precursors by dip-coating lacks the control of thickness. Lee *et al.* [17] chose MoO_3 powder as precursor for CVD growth of MoS_2 thin films by seeding the substrate with reduced graphene oxides. The resulting product may have contamination of the seeds. Recently, Yu *et al.* [18] reported a self-limiting CVD approach to produce large-area MoS_2 thin films on various substrates but a very low carrier mobility (0.003–0.03 $cm^2\ V^{-1}\ s^{-1}$) was achieved.

In this work, we report a seedless and scalable growth method using ambient pressure CVD to produce high quality few-layer MoS_2 thin film. Compared with previous reports which used low-pressure CVD to grow MoS_2 [18,19], the present method has simpler operation procedures and better repeatabilities. The as-grown MoS_2 on SiO_2/Si is suitable for following device fabrication without transfer process which could induce defects and impurities. The scalable growth method can be further adopted to more complicated photonic structures such as waveguides and gratings, affording compatability with integrated photonic circuits.

2. RESULTS AND DISCUSSION

Figure 1(a) schematically shows the experimental setup to synthesize MoS_2 thin film on SiO_2 substrate. The sulfur powder was located at upstream of the CVD system. The MoO_3 powder was placed in a quartz boat in the furnace and the SiO_2 substrate was next to the MoO_3 source. During the growth, sulfur and MoO_3 were heated to 100°C and 650°C, respectively. The carrying gas argon was at a flow rate of 150 sccm and the system was kept at ambient pressure. As illustrated in Fig. 1(a), MoO_3 is reduced by sulfur vapor to form MoO_{3-x} species [17,20], which will diffuse to SiO_2 substrate and eventually lead to nucleation and growth of MoS_2 thin film.

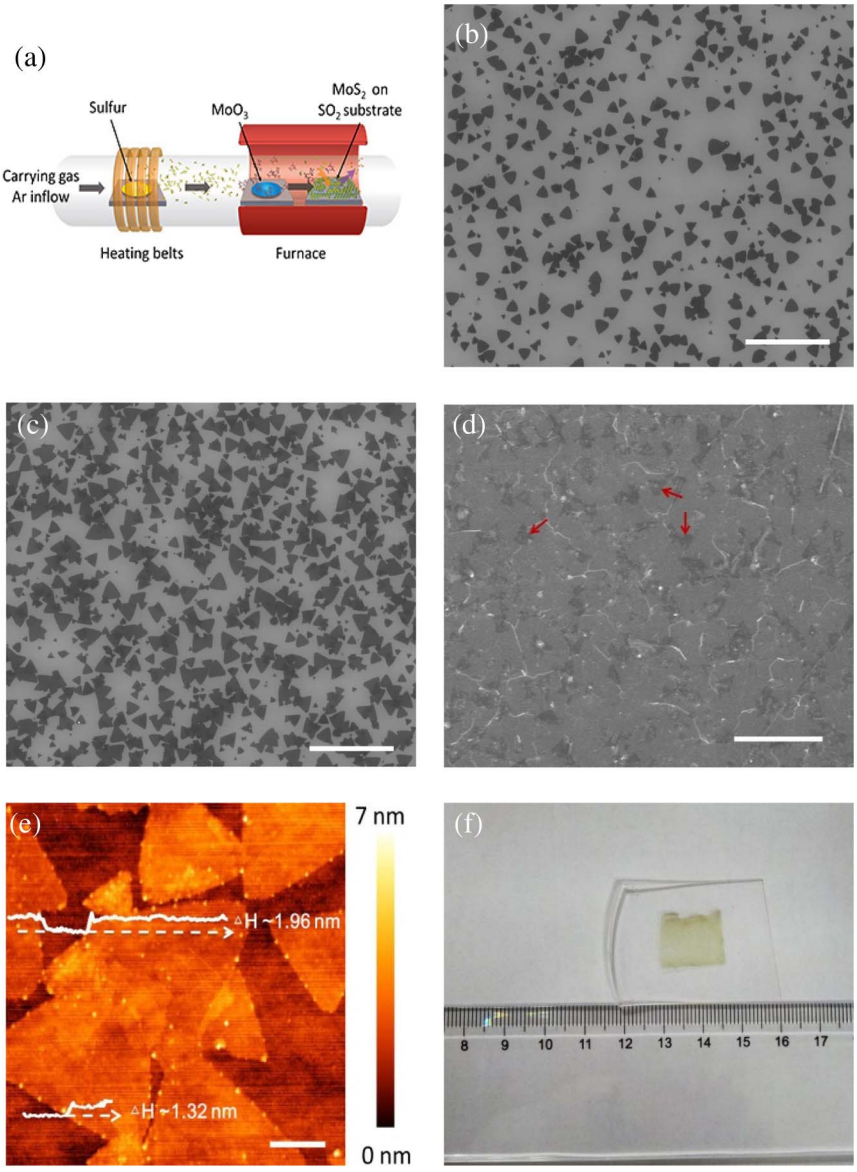

Fig. 1. Material characterizations of MoS_2; (a) schematic diagram showing the chemical synthesis of MoS_2; (b–d) SEM images showing different growth stages of MoS_2 with different reaction times of 5, 12, and 30 min, respectively. Scale bars, 10 μm; (e) AFM topography of MoS_2 film on SiO_2 substrate. Bottom and top white profiles indicate bilayer and trilayers, respectively. Scale bar, 1 μm; (f) optical image of large-area MoS_2 film transferred onto PDMS substrate.

Figures 1(b)–1(d) show scanning electron microscope (SEM) images of MoS_2 films with different morphologies. The growth times are 5, 12, and 30 min for Figs. 1(b), 1(c), and 1(d), respectively, with the same growth temperature of 650°C. It is found that these samples represent different growth stages. At the early stage of growth, the triangle-shaped MoS_2 crystals randomly distribute on SiO_2 substrate, as shown in Fig. 1(b). Upon prolonging the growth time to 12 min, smaller grains turn into larger ones by adsorbing atoms, as indicated in Fig. 1(c). It should be noted that the crystals tend to interconnect rather than overlap with each other when they grow larger. When the growth time is prolonged to 30 min, full coverage of MoS_2 film was achieved due to the coalescence of large crystals, as shown in Fig. 1(d). The uniformity is verified by the small difference in the contrast over the whole film. The white color lines mainly correspond to gaps among crystals. When MoS_2 film is fully covered on the substrate, incoming MoS_2 species will nucleate to form thicker triangle crystals (as indicated by the red arrows), whereas a small portion of them will aggregate to form curved nanoparticles or quasi-one-dimensional nanowires.

Figure 1(e) shows the representative atomic force microscopy (AFM) topography of MoS_2 film on SiO_2 substrate. It reveals a few triangular domains interconnecting with each other. The homogeneous color contrast indicates good uniformity. The line profiles indicate thickness of about 1.32 and 1.96 nm, corresponding to bilayer [18] and trilayer MoS_2 film [21]. The few-layer MoS_2 thin film grown on SiO_2 substrate can be completely peeled off and transferred to other arbitrary substrates. Figure 1(f) shows a centimeter-size MoS_2 film which was transferred onto polydimethylsiloxane (PDMS) film with good continuity.

Spectroscopic characterizations were carried out to evaluate the quality of MoS_2 film. Figure 2(a) shows Raman spectra

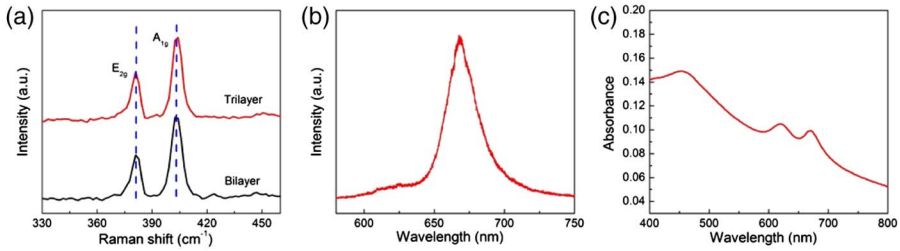

Fig. 2. Spectroscopic characterizations of MoS_2 films; (a) Raman spectra of few-layer MoS_2 on SiO_2/Si substrate; (b) PL spectrum of few-layer MoS_2 film; (c) UV–visible spectrum of few-layer MoS_2 film on quartz.

of the as-grown MoS_2 film measured at the excitation of 514 nm, which reveals two characteristic peaks. The peak is around 380 cm^{-1} attributed to the in-plane E_{2g} mode resulting from opposite vibration of two S atoms with respect to the Mo atom. The peak is around 400 cm^{-1} assigned to the A_{1g} mode which is associated with the out-of-plane vibration of only S atoms in the opposite directions [22,23]. The frequency difference (Δ) between E_{2g} and A_{1g} increases with the thickness, which can be used to identify the number of layer in atomic layered MoS_2 [16,20,24]. In this context Δ is calculated to be $\sim$21.5 and 22.9 cm^{-1}, corresponding to bilayer and trilayer MoS_2 film, respectively [21,22]. Figure 2(b) shows the photoluminescence (PL) spectrum (with 514 nm laser excitation) which also consists of two pronounced emission peaks at around 625 and 670 nm. The strong light emission corresponds to the direct excitonic transitions at the Brillouin zone K point [20]. The appearance of these two emission peaks is in consistent with two excitonic absorption bands around 620 and 670 nm shown in the UV–visible spectrum [Fig. 2(c)].

Transmission electron microscopy (TEM) is also employed to characterize the quality and crystal structure of transferred MoS_2 film. Figure 3(a) shows the microstructure of a piece of MoS_2 film folded on TEM grid. The high-resolution TEM (HRTEM) image clearly resolves the lattice of few-layer MoS_2 film. The selected area electron diffraction (SAED) pattern in the inset of Fig. 3(b) contains multi-group 6-fold symmetry spots, which indicates that the measured zone of MoS_2 film contains several grains possessing different crystal orientations. Meanwhile, the X-ray photoelectron spectroscopy (XPS) results shown in Fig. 3(c) reveal the binding energies of Mo-3$d_{3/2}$ and Mo-3$d_{5/2}$ at 232.5 and 229.3 eV, respectively. Two peaks located at 163.2 and 162.0 eV are attributed to S-2$p_{1/2}$ and S-2$p_{3/2}$, respectively. These binding energy results are in good consistent with previous reports [25,26], suggesting the successful growth of layered MoS_2 film. The X-ray diffraction (XRD) profile for few-layer MoS_2 is shown in Fig. 3(d). The diffraction peaks at 14.4° and 33.1° are attributed to the (002) and (100) crystal planes, respectively [6,16].

To investigate the electrical performance of our sample, we fabricated back gate field-effect transistors using few-layer MoS_2 directly grown on SiO_2/Si substrate. The typical transfer

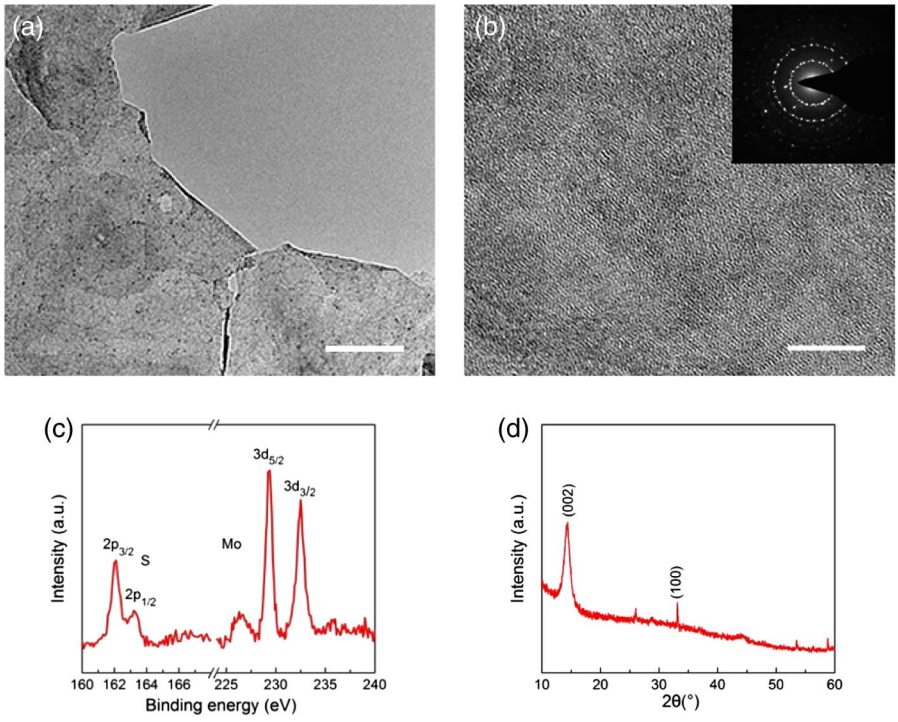

Fig. 3. (a) TEM image showing folded MoS_2 film. Scale bar, 100 nm; (b) HRTEM image of MoS_2 film. Scale bar, 5 nm. Inset, corresponding electron diffraction pattern; (c) XPS spectrum of MoS_2 thin film; (d) XRD result for MoS_2 thin film.

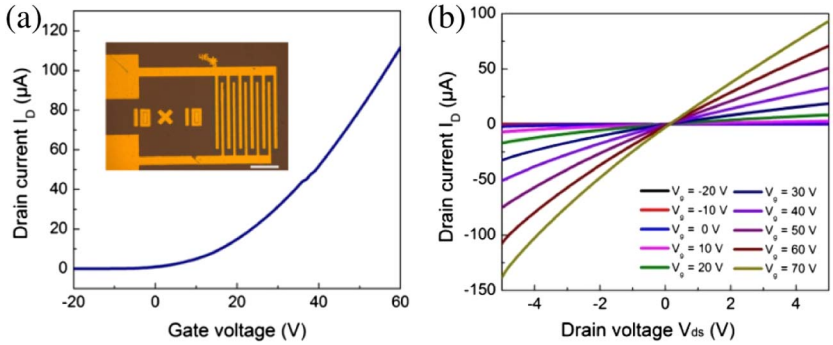

Fig. 4. (a) Typical transfer curve for MoS_2 transistor. Inset, optical image of a FET device. Scale bar, 100 μm; (b) output curve for MoS_2 transistor.

I_d versus V_g curve of MoS_2 transistor device is shown in Fig. 4(a). We can extract the device on-off ratio up to 10^5, which is sufficiently high for transistor device based on few-layer MoS_2 considering that back gate structure was used. Furthermore, the calculated field effect carrier mobility turns out to be 3.4 $cm^2\ V^{-1}\ s^{-1}$ via $\mu = \frac{dI_D}{dV_g}\ \frac{L}{W}\ \frac{d}{\varepsilon}\ \frac{1}{V_D}$, where ε is the dielectric constant of SiO_2; L and W are the channel length and channel width, respectively. It is worth noting that the room temperature carrier mobility of our device is comparable to that based on monolayer MoS_2 with the similar configuration, which are usually in the range of 0.1–10 $cm^2\ V^{-1}\ s^{-1}$ [27,28]. Figure 4(b) shows output characteristics of the few-layer MoS_2 device. It is seen that the drain current is dependent on the drain–source voltage at various back-gate voltages, which implies good gate tunability of our device.

3. CONCLUSION

In summary, we have successfully developed a facile method to grow large-area MoS_2 on SiO_2/Si substrate via ambient pressure CVD. The material characterization results show that our MoS_2 films are mainly two to three atomic layers with good uniformity and high quality. The few-layer MoS_2 thin film show good electrical properties, i.e., the mobility of our MoS_2 transistor is comparable to that of transistors based on monolayer MoS_2 flakes. Our work provides a route toward scalable growth of high-quality few-layer MoS_2 film and the MoS_2 thin films are ideal materials for electronics and optoelectronic devices.

4. EXPERIMENTAL SECTION

A. Materials Synthesis

The MoS_2 films were synthesized on SiO_2/Si substrates (SiO_2 thickness, 300 nm) via CVD technique. The substrates were cleaned in acetone and isopropanol successively. Prior to the growth, argon gas (99.999%) was used to clean the growth chamber at room temperature. High-purity MoO_3 (99.5%, Alfa Aesar) and sulfur powder (99.5%, Sinopharm Chemical Reagent, Shanghai Co., Ltd.) were kept in two separate quartz boats in the furnace with the substrates placed downstream of the CVD system. For the growth of MoS_2, the furnace was heated up to 650°C and maintained for 30 min, while the argon gas was purging with a flow rate of 150 sccm at ambient pressure. Afterward, the furnace was cooled down naturally to room temperature.

B. Material Characterization

Raman and PL spectra were collected by micro-Raman system (Horiba Jobin Yvon, HR800). The excitation wavelength is 514 nm, and the laser spot is focused to <2 μm with 100× objective lens. UV-visible absorption spectra were obtained by UV-visible-IR spectrometer (PerkinElmer, Lambda750 system). Chemical composition and crystal orientation were studied using XPS (KRATOS Analytical, KRATOS AXIS Ultra DLD) and XRD (PANPANalytical B.V.P, Ruki). Surface morphology of the samples was examined by SEM (FEI, Quanta 200 FEG) and AFM (Bruker, Dimension Icon). TEM (FEI, Tecnai G2 F20) was used to investigate the microstructures.

C. Fabrication of Transistors

The transistor devices were directly fabricated on MoS_2 films grown on SiO_2/Si substrates. The highly doped n-type silicon of SiO_2/Si substrate serves as the back-gate electrode. The device fabrication includes UV lithography to define the device pattern and electron-beam evaporation to deposit source and drain electrodes (100 nm Au on top of 5 nm Ti).

D. Electrical Measurements

The measurements were performed by probe station (Cascade M150) equipped with a semiconductor property analyzer (Keithley 2400) at room temperature in ambient conditions.

ACKNOWLEDGMENTS

We acknowledge the support from the National High Technology Research and Development Program of China (863 Program) (Grant No. 2013AA031903), the Youth 973 Program (Grant No. 2015CB932700), the National Natural Science Foundation of China (Grant Nos. 91433107, 51222208, and 51290273), the Doctoral Fund of Ministry of Education of China (Grant No. 20123201120026), ARC DP (DP140101501), ARC DECRA (DE120101569), and Victoria DSI top-up grant. S. Li acknowledges the support from the Natural Science Foundation of Jiangsu Province (No. BK20130328), China Postdoctoral Science Foundation (No. 2014M551654), and Jiangsu Province Postdoctoral Science Foundation (No. 1301020A).

REFERENCES

1. D. Lembke and A. Kis, "Breakdown of high-performance monolayer MoS_2 transistors," ACS Nano **6**, 10070–10075 (2012).

2. H. Schmidt, S. Wang, L. Chu, M. Toh, R. Kumar, W. Zhao, A. H. Castro Neto, J. Martin, S. Adam, and B. Özyilmaz, "Transport properties of monolayer MoS_2 grown by chemical vapor deposition," Nano Lett. **14**, 1909–1913 (2014).
3. B. W. Baugher, H. O. Churchill, Y. Yang, and P. Jarillo-Herrero, "Intrinsic electronic transport properties of high-quality monolayer and bilayer MoS_2," Nano Lett. **13**, 4212–4216 (2013).
4. A. Splendiani, L. Sun, Y. Zhang, T. Li, J. Kim, C.-Y. Chim, G. Galli, and F. Wang, "Emerging photoluminescence in monolayer MoS_2," Nano Lett. **10**, 1271–1275 (2010).
5. B. Radisavljevic, A. Radenovic, J. Brivio, V. Giacometti, and A. Kis, "Single-layer MoS_2 transistors," Nat. Nanotechnol. **6**, 147–150 (2011).
6. S. Balendhran, J. Z. Ou, M. Bhaskaran, S. Sriram, S. Ippolito, Z. Vasic, E. Kats, S. Bhargava, S. Zhuiykov, and K. Kalantar-Zadeh, "Atomically thin layers of MoS_2 via a two step thermal evaporation-exfoliation method," Nanoscale **4**, 461–466 (2012).
7. M. Chhowalla, H. S. Shin, G. Eda, L. J. Li, K. P. Loh, and H. Zhang, "The chemistry of two-dimensional layered transition metal dichalcogenide nanosheets," Nat. Chem. **5**, 263–275 (2013).
8. K. Kaasbjerg, K. S. Thygesen, and K. W. Jacobsen, "Phonon-limited mobility in n-type single-layer MoS_2 from first principles," Phys. Rev. B **85**, 115317 (2012).
9. S. Ghatak, A. N. Pal, and A. Ghosh, "Nature of electronic states in atomically thin MoS_2 field-effect transistors," ACS Nano **5**, 7707–7712 (2011).
10. H. Liu, A. T. Neal, and P. D. Ye, "Channel length scaling of MoS_2 MOSFETs," ACS Nano **6**, 8563–8569 (2012).
11. H. Hwang, H. Kim, and J. Cho, "MoS_2 nanoplates consisting of disordered graphene-like layers for high rate lithium battery anode materials," Nano Lett. **11**, 4826–4830 (2011).
12. Y. Yao, Z. Lin, Z. Li, X. Song, K.-S. Moon, and C.-P. Wong, "Large-scale production of two-dimensional nanosheets," J. Mater. Chem. **22**, 13494–13499 (2012).
13. J. N. Coleman, M. Lotya, A. O'Neill, S. D. Bergin, P. J. King, U. Khan, K. Young, A. Gaucher, S. De, and R. J. Smith, "Two-dimensional nanosheets produced by liquid exfoliation of layered materials," Science **331**, 568–571 (2011).
14. S. Wu, C. Huang, G. Aivazian, J. S. Ross, D. H. Cobden, and X. Xu, "Vapor-solid growth of high optical quality MoS_2 monolayers with near-unity valley polarization," ACS Nano **7**, 2768–2772 (2013).
15. Y. Zhan, Z. Liu, S. Najmaei, P. M. Ajayan, and J. Lou, "Large-area vapor-phase growth and characterization of MoS_2 atomic layers on a SiO_2 substrate," Small **8**, 966–971 (2012).
16. K. K. Liu, W. Zhang, Y. H. Lee, Y. C. Lin, M. T. Chang, C. Y. Su, C. S. Chang, H. Li, Y. Shi, and H. Zhang, "Growth of large-area and highly crystalline MoS_2 thin layers on insulating substrates," Nano Lett. **12**, 1538–1544 (2012).
17. Y. H. Lee, X. Q. Zhang, W. Zhang, M. T. Chang, C. T. Lin, K. D. Chang, Y. C. Yu, J. T. W. Wang, C. S. Chang, and L. J. Li, "Synthesis of large-area MoS_2 atomic layers with chemical vapor deposition," Adv. Mater. **24**, 2320–2325 (2012).
18. Y. Yu, C. Li, Y. Liu, L. Su, Y. Zhang, and L. Cao, "Controlled scalable synthesis of uniform, high-quality monolayer and few-layer MoS_2 films," Sci. Rep. **3**, 1866 (2013).
19. J. Zhang, H. Yu, W. Chen, X. Tian, D. Liu, M. Cheng, G. Xie, W. Yang, R. Yang, and X. Bai, "Scalable growth of high-quality polycrystalline MoS_2-monolayers on SiO_2 with tunable grain sizes," ACS Nano **8**, 6024–6030 (2014).
20. Q. Ji, Y. Zhang, T. Gao, Y. Zhang, D. Ma, M. Liu, Y. Chen, X. Qiao, P.-H. Tan, and M. Kan, "Epitaxial monolayer MoS_2 on mica with novel photoluminescence," Nano Lett. **13**, 3870–3877 (2013).
21. D.-S. Tsai, K. K. Liu, D. H. Lien, M. L. Tsai, C. F. Kang, C. A. Lin, L. J. Li, and J. H. He, "Few-layer MoS_2 with high broadband photogain and fast optical switching for use in harsh environments," ACS Nano **7**, 3905–3911 (2013).
22. H. Li, Q. Zhang, C. C. R. Yap, B. K. Tay, T. H. T. Edwin, A. Olivier, and D. Baillargeat, "From bulk to monolayer MoS_2: Evolution of Raman scattering," Adv. Funct. Mater. **22**, 1385–1390 (2012).
23. X. Zhang, W. Han, J. Wu, S. Milana, Y. Lu, Q. Li, A. Ferrari, and P. Tan, "Raman spectroscopy of shear and layer breathing modes in multilayer MoS_2," Phys. Rev. B **87**, 115413 (2013).
24. H. Li, Z. Yin, Q. He, H. Li, X. Huang, G. Lu, D. W. H. Fam, A. I. Y. Tok, Q. Zhang, and H. Zhang, "Fabrication of single-and multilayer MoS_2 film-based field-effect transistors for sensing no at room temperature," Small **8**, 63–67 (2012).
25. X. Wang, H. Feng, Y. Wu, and L. Jiao, "Controlled synthesis of highly crystalline MoS_2 flakes by chemical vapor deposition," J. Am. Chem. Soc. **135**, 5304–5307 (2013).
26. C. Altavilla, M. Sarno, and P. Ciambelli, "A novel wet chemistry approach for the synthesis of hybrid 2D free-floating single or multilayer nanosheets of MS_2 @ oleylamine (M, Mo, W)," Chem. Mater. **23**, 3879–3885 (2011).
27. K. Novoselov, D. Jiang, F. Schedin, T. Booth, V. Khotkevich, S. Morozov, and A. Geim, "Two-dimensional atomic crystals," Proc. Natl. Acad. Sci. USA **102**, 10451–10453 (2005).
28. J. Lin, J. Zhong, S. Zhong, H. Li, H. Zhang, and W. Chen, "Modulating electronic transport properties of MoS_2 field effect transistor by surface overlayers," Appl. Phys. Lett. **103**, 063109 (2013).